ISAC CYTOMETRY Journal of Quantitative Cell Science PART A

MIFlowCyt

An Evaluation of T-Cell Functionality After Flow Cytometry Sorting Revealed p38 MAPK Activation

Immanuel Andrä,[1] Hanna Ulrich,[2] Susi Dürr,[1] Dominik Soll,[1] Lynette Henkel,[1] Corinne Angerpointner,[1] Julia Ritter,[2] Sabine Przibilla,[3] Herbert Stadler,[4,5] Manuel Effenberger,[1] Dirk H. Busch,[1,6,7] Matthias Schiemann[1*]

[1]Institute for Medical Microbiology, Immunology and Hygiene, Technische Universität München (TUM), Munich, Germany

[2]Institute for Systemic Inflammation Research, Universität zu Lübeck, Lübeck, Germany

[3]Juno Therapeutics GmbH, Munich, Germany

[4]Cell.Copedia GmbH, Leipzig, Germany

[5]IBA GmbH, IBA Lifesciences, Göttingen, Lower SaxonyGermany

[6]Focus Group 'Clinical Cell Processing and Purification', Institute for Advanced Study, TUM, Munich, Germany

[7]National Centre for Infection Research (DZIF), Munich, Germany

Received 2 May 2019; Revised 4 December 2019; Accepted 9 December 2019

Grant sponsor: Research Foundation, Grant number: 272983813; Grant sponsor: Deutsche Forschungsgemeinschaft

Additional Supporting Information may be found in the online version of this article.

*Correspondence to: Matthias Schiemann, Institute for Medical Microbiology, Immunology and Hygiene, Technische Universität München (TUM), Trogerstrasse 30, 81675 München, Germany Email: matthias.schiemann@tum.de

Published online 16 January 2020 in Wiley Online Library (wileyonlinelibrary.com)

ISAC INTERNATIONAL SOCIETY FOR ADVANCEMENT OF CYTOMETRY

Abstract

Cell alterations during isolation and preparation for flow cytometry cell sorting by antibodies, temperature, homogenization, buffer composition and mitogens are well known. In contrast, little is known about cell alteration caused by the instrument or the sorting process itself. We systematically evaluated cellular responses to different sorter-induced physical forces. In summary, flow cytometry cell-sorting induced forces can affect cellular signaling cascades, especially the MAPK p38. Functional assays, related to the p38 MAPK pathway, of human primary T cells after flow cytometry sorting did lead to minor physiological modulation but no functional impairments.

Key terms

flow cytometry cell sorting; cell sorting; MAPK; p38 activation; T cells; cell purification; cell stress; traceless affinity cell selection

Cellular Stress Signaling

Activation of cells by external stress factors is a conserved mechanism across taxonomic kingdoms including plants, fungi, and animals and is often mediated by the mitogen-activated protein kinase (MAPK) pathways (1). Four major MAPK nodes have been described that can be activated separately depending on the stimuli (Supporting Information Fig. S1A). Extracellular-signaling-regulated kinases 1 and 2 (Erk1/2) react to varieties of extracellular stimuli; extracellular-signaling-regulated kinase 5 (Erk5) is known for being activated by stress signals like oxidative stress, hyperosmolarity, or mitogens (2); a main function of the c-Jun-amino-terminal kinase (JNK) is to respond on osmotic shock, ultraviolet irradiation, or heat shock. And finally, the p38 family consisting of four different members (α, β, γ, and δ, where the α-p38 is ubiquitously expressed in nearly all tissues) responds to environmental factors and inflammation.

MAPK are one possible way for cell stress signaling, another well described response to stress is mediated by the eukaryotic initiation factor 2 (eIF2) (3). This protein is phosphorylated via different serine kinases by various activating stimuli in its alpha unit, which leads to a stop in mRNA translation (Supporting Information Fig. S2A).

Cell Alteration by Preparation and Purification

The separation of heterogeneous samples into defined subpopulations is indispensable for the evaluation of individual cells types in *in vitro* and *in vivo* studies (4–6). Of all cell separation technologies, purification by antibody binding offers the highest purity and specificity. The two key technologies of antibody-based cell separation are bead-based cell sorting and flow cytometry cell sorting. Both methods can potentially lead to cell stress or cell alteration, whereby sample preparation is the first contributing factor. For example, the use of different buffers leads to changes in

DOI: 10.1002/cyto.a.23964

osmolarity (7–9), changes pH, or adds traces of mitogens (10). Additionally, solid tissues or blood derived material require cell homogenization (11), collagenase digestion (12), or the use of anticoagulants like heparin (13); all of them expose cells to considerable stress. Furthermore, certain antibodies alter cell physiology and function by receptor stimulation, blockade (14–17), or through initiation of cell- or complement-mediated cell lysis (18). First efforts made to reduce antibody effects included the use of reversible antibodies (19), which in turn required handling cells at low temperatures in order to prevent signaling, internalization, and cell lysis. In this regard, studies have already shown that hypothermal working temperatures have a significant impact on protein synthesis (20), induce pathways via eIF2α, and further might induce MAPK cell signaling (21). Despite these challenges in sample preparation, antibody-based cell separation remains an indispensable tool in basic research for life sciences and clinical cell-based therapies.

Antibody-Based Cell Separation Methods

Bead based and/or magnetic separation is associated with high purity, yield, and recovery of large cell numbers. It can be easily combined with other purification methods (22) and has already been used for various clinical applications (23–25). This method requires only low technological prerequisites concerning instrumentation and training.

In contrast, flow cytometric cell sorting is considerably more complicated but offers the opportunity to investigate multiple markers in parallel on single-cell level as well as providing higher purity and yields than magnetic separations.

However, mechanisms fundamental to the method of flow cytometry cell sorting itself (Fig. 1) potentially could affect cell phenotypes and cell functionalities. The biological status of cells, their viability, vitality, and functionality after a sort is crucial for the validity and outcome of subsequent experiments and has to be evaluated. So far published work (12,26) on instrument-induced changes use either harsh cell preparation processes or reporter proteins in immortalized cell culture, so that both systems suffered under pre-experimental cellular alterations. In this study, we specifically focused on the identification of cell changes caused by the sorting process, highlighting mechanical and physical forces potentially detrimental.

Material and Methods

Chemicals and Disposables

If not mentioned separately disposables were purchased from Greiner Bio-One GmbH (Frickenhausen, Germany) and all chemicals were ultra-pure grade (Sigma, Heidelberg, Germany).

Isolation of Human Peripheral Blood Mononuclear Cell

Human peripheral blood mononuclear Cells (PBMCs) were isolated in Leucosep™ Tubes by density centrifugation with Biocoll Separating Solution from fresh heparinized venous blood of healthy donors or buffy coats, obtained from healthy individuals during blood donation (German Heart Centre Munich, Munich, Germany). Blood donations were obtained from voluntary donors after informed consent under regulatory conditions and in accordance with the declaration of Helsinki (27). PBMCs were kept at 37°C with 5% CO_2 in RPMI-1640 containing 10% fetal calf serum (FCS) and 50 k units of penicillin, 50 mg streptomycin for cell culture or 2% FCS for MAPK-signaling assays.

Isolation of Murine Splenocytes

Wild-type C57BL/6 mice (Envigo RMS GmbH, Leppsteinswiesen, Germany) were sacrificed by cervical dislocation at an age of 8–10 weeks, in agreement with the rules of the regulatory authority "Regierung von Oberbayern." Spleens were homogenized with a cell strainer and red blood cell lysis was done with tris-buffered ammonium chloride (ACT) containing 170 mM NH_4Cl and 220 mM TrisHCl. Splenocytes were cultured in 50% Dulbecco's Modified Eagle's Medium (DMEM) and 50% RPMI-1640 containing 0.025% L-Glutamine, 10% FCS, 1% PenStrep, and β-mercaptoethanol (0.1%).

Cell Culture Conditions for Immortalized Cells

Adherent cell lines were cultured in DMEM with 0.025% L-Glutamine, 10% FCS, and 1% PenStrep. Suspension cells were cultured in RPMI-1640 with 0.025% L-Glutamine, 10% FCS, and 1% PenStrep.

Fab-TACS® Traceless Affinity Cell Selection

Fab-TACS® columns (IBA Lifesciences, Göttingen, Germany) for 10 ml human whole blood or Buffy Coat material were equilibrated with 10 ml of staining buffer (PBS with 0.5% [w/v] BSA and 1 mM EDTA, pH 7.4) and coated two times with 30 μg CD8 Fab (IBA Lifesciences, Göttingen, Germany) dissolved in 3 ml of staining buffer. Attached cells were dissolved from the matrix by running 5 ml of staining buffer containing 100 mM D-Biotin. Eluted fraction was washed in 50 ml of staining buffer. Purity, depletion, and viability of sample material were determined by flow cytometry with CD8 Allophycocyanin (APC), CD3 Brilliant Violet 650 (BV650), CD235 Phycoerythrin (PE), and propidium iodide (PI; ThermoFischer Scientific, Waltham) 1 μg/ml.

Cell Sorting

For cell sorting, the MoFlo™ legacy, MoFlo™ XDP (Beckman Coulter, Inc., Fullerton), S3e™ (BIO-RAD

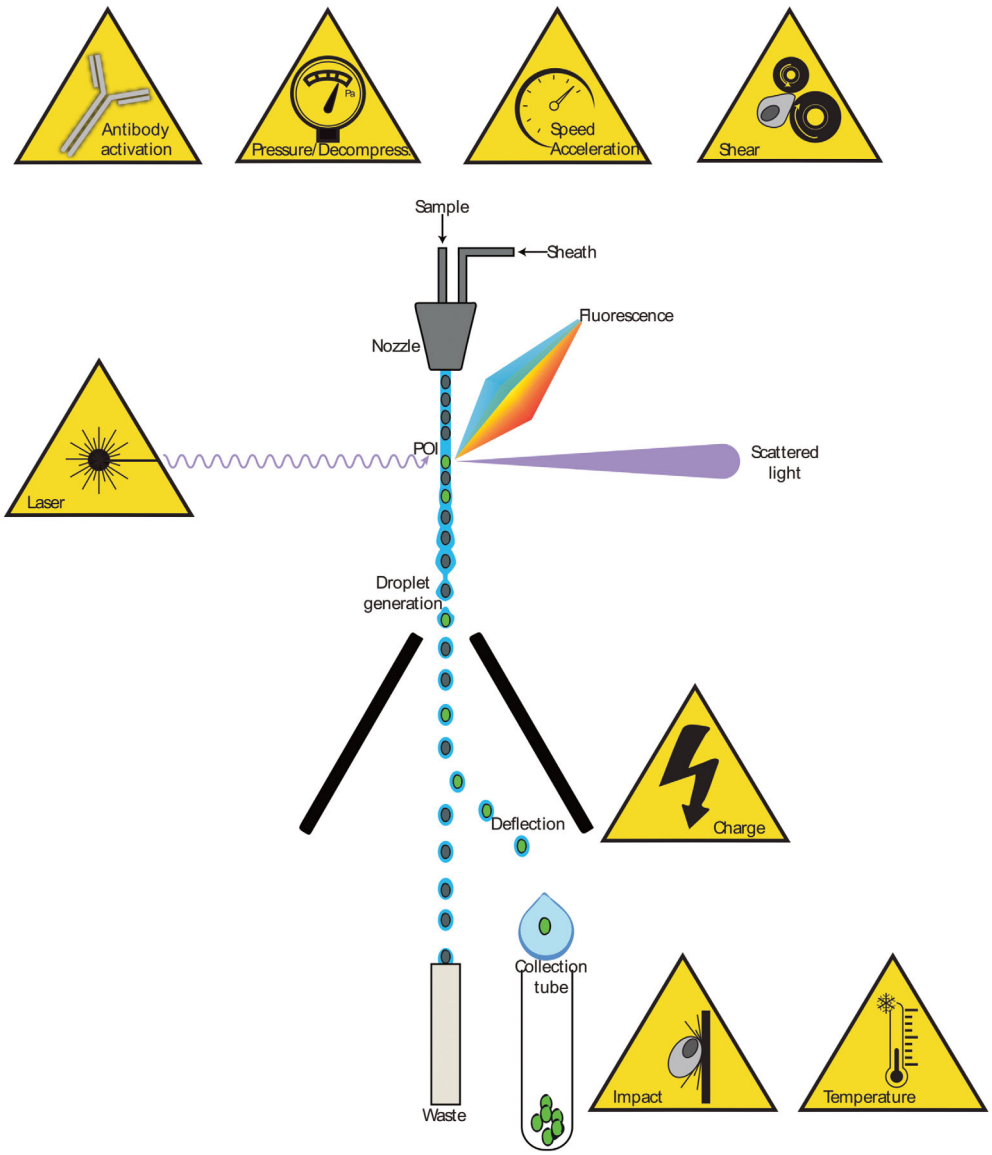

Figure 1. A "jet in air" flow cytometry cell sorter layout highlighting physical forces and risks of biological changes due to sample preparation and cell sorting.

laboratories GmbH, Munich, Germany) or FACSAria™ III (BD Bioscience, Franklin Lakes) were used. When flow cytometry instruments were compared a 100 µm nozzle was used at 30 psi. If not specified elsewhere, samples at a concentration of 1×10^7 cells/ml were sorted with a sample pressure of 60 psi, a 70 µm nozzle, and a maximum event rate of 20,000 events per second (eps).

Staining Procedures

Staining was done in the dark at 4°C with staining buffer for 20 min.

Prior to intracellular phosphoprotein staining, 2 µg/ml ethidium monoazide (EMA) was incubated with staining buffer containing NaN_3 0.06% (v/v) under light exposure for 20 min. Cells were then fixed by adding 2% final concentration PFA at RT for 20 min. After the addition of 250 µl of methanol (99%) at 4°C and 20 min incubation cells were washed and stained with p-JNK PE (CellSignaling, Danvers), p-Erk1/2_Peridinin-Chlorophyll-protein-eFluor710 (PerCPeF710) and p-p38 APC (ThermoFischer Scientific). After two washing steps, cells were analyzed.

Western Blotting

Cytoplasmic lysates were generated by incubation for 15 min on ice in 50 µl of NP-40 buffer containing 50 mM HEPES, 40 mM NaCl, 1 mM DTT, 1 mM Na_2EDTA, 1 mM EGTA, 0.5% (v/v) Nonident P-40, 10% (v/v) glycerol, 20 mM β-glycerolphosphate, 1 mM Na_3VO_4, 0.4 mM PMSF, 1 mM NaF, 1 tablet of protease inhibitor (Roche Diagnostics GmbH, Mannheim, Germany) adjusted to pH 7.6. Cell debris was removed by centrifugation. Supernatant was heated at 95°C

with 4*Lämmli buffer 62,5 mM Tris, 2% SDS, 50% glycerol, 2 mM EDTA, 1% bromphenolblue, and 100 mM DTT for 5 min. The 10% SDS-polyacrylamidgels were used for gelelectrophoresis, running at 120 V for 100 min with running buffer 25 mM tris, 3.5 mM SDS, 200 mM glycine with a protein size-ladder 10–170 kDA (peqlab, Erlangen, Germany). Incubation with specific rabbit antibodies p-p38, endogenous p38, p-Erk1/2, p-Erk5, p-eIF2α, and β-actin (CellSignaling, Danvers) was done. Signals were detected by mouse-α-rabbit IgG coupled to HRP (CellSignaling), and WesternLightning ECL substrate (Perkin Elmer Inc., Waltham).

RNA Isolation

RNA was extracted with the RNeasy Micro Kit (Qiagen GmbH, Hilden, Germany), according to distributer's protocol. After drying columns were stored at −80°C until all time points were acquired. mRNA was eluted from columns with 14 µl RNase free H_2O and stored at −80°C until MicroArray analysis. mRNA yield was measured with NanoDrop ND-1000 (Nanodrop, Steinfurt, Germany).

MicroArray and Data Analysis

mRNA quality was determined with Experion RNA Chips (BIO-RAD laboratories GmbH, Munich, Germany). RNA concentration ranged from 85 ng/µl to 124 ng/µl with a ratio of 28S/18S for the ribosomal RNA ranging from 1.06 to 2.58. The RQI for all samples was between 8.2 and 9.1. mRNA was translated into DNA, fragmented and labeled and MicroArray analysis was done with the Affimetrix™ (ThermoFischer Scientific) using the Gene Chip™ Human Gene 1.0 ST (ThermoFischer Scientific).

Survival and Apoptosis

Living cells were determined with PI (1 µg/ml), EMA (2 µg/ml), 7-Aminoactinomycin D (7AAD), Flica-Cell event green_ Fluorescein_isothiocyanate (FITC), and AnnexinV_PacificBlue (PB; ThermoFischer Scientific) staining. AnnexinV binding buffer contained 140 mM NaCl, 4 mM KCl, 0.75 mM $MgCl_2$, and 10 mM HEPES. Staining for early apoptotic markers was done with FLICA at room temperature in the dark for 30 min with subsequent washing steps before staining with 7AAD and AnnexinV in AnnexinV binding buffer. For viability approaches with PI staining PBS buffer was used. Parallel sorting with identical samples at the same time were performed on all instruments with matching instrument setup criteria.

Migration

PBMCs were stained with CD4, CD14, CD16, CD19, on ECD. Samples were divided into alternate CD8 staining with the fluorochromes PB and PE to control for staining-induced differences in migration. Migration assay was done in Costar® 24 well Transwell® plates (Corning Incorporated, Kennebunk) pore size 5 µm. The 2×10^5 cells ("mock" and unsorted equally) were added per well, in RPMI medium without additives. Chemotaxis was established by RPMI containing 1% FCS in the lower plate.

Proliferation - Mixed Lymphocyte Reaction

From human PBMCs 2.5×10^5 effector cells HLA-mismatched together with 1×10^5 γ-irradiated (30 Gy) stimulator cells were harvested by a Micro96 Harvester (Skatron Instruments, Woonsocket) and transferred from a 96-well plate onto glass fiber filters. A beta counter 1500TR (ThermoFischer Scientific) detected emitted electrons from 3H-Thymidine (Hartmann Analytik GmbH, Braunschweig, Germany) taken up by proliferating cells. Cells were incubated with a total of 1 µCi per well. MLR experiments were sorted with a 100 µm nozzle at 30 psi.

Antigen-Specific Killing

TCR transgenic T cells recognizing the MART-$1_{(A27L)\ 26-35}$ epitope were sorted by flow cytometry based on CD8 and pMHC positivity and subsequently expanded using 1.0 µg/ml αCD3, 0.5 µg/ml αCD28 antibodies (BD Bioscience, Franklin Lakes) and 50 U/ml IL2 (Peprotech, Hamburg,Germany).

The 5×10^3 A375 melanoma cells (28) were grown to confluency within a 96-well E-plate at 37°C and 5% CO_2. Baseline growth was monitored within the xCELLigence system (ACEA, San Diego). A375 pulsing was done in 100 µl growth medium containing 10^{-7} M MART-1 peptide for 60 min. Culture medium was replaced with 100 µl RPMI containing 5% human serum, 1% PenStrep, 1% sodium pyruvate, and MART-1 effector T cells (either "mock" sorted or sort-medium exchanged) ranging in numbers from 1:1 to 8:1 E:T ratio. All conditions were done in duplicates; while killing was quantified by measuring impedance every 15 min for 48 h. Specific cell lysis was calculated from cell indices in a total of $n = 4$ experiments:

$$\text{Specific lysis} = \frac{n\text{CI}(\text{A375 only}) - n\text{CI}(\text{A375sample})}{n\text{CI}(\text{A375only})}$$

Statistical Methods

For cell migration experiments replicates of $n = 6$ for each condition were measured as a percentage of migrated $CD8^+$ cells. Two-way ANOVA comparison of sorted and unsorted conditions gave a p-value of 0.2714 for observing sorting-induced effects. Mainly labeling color and incubation time affected the percentage of migrated CD8 cells with a p value of <0.0001.

MLR experiments were done in replicates of $n = 8$. Data were analyzed using two-tailed unpaired t test comparing purification conditions to unsorted material.

MicroArray data ($n = 2$) were RMA normalized which included a log2 transformation. mRNA upregulation was determined by:

$$A - B > 1 \rightarrow \frac{2^A}{2^B} > 2$$

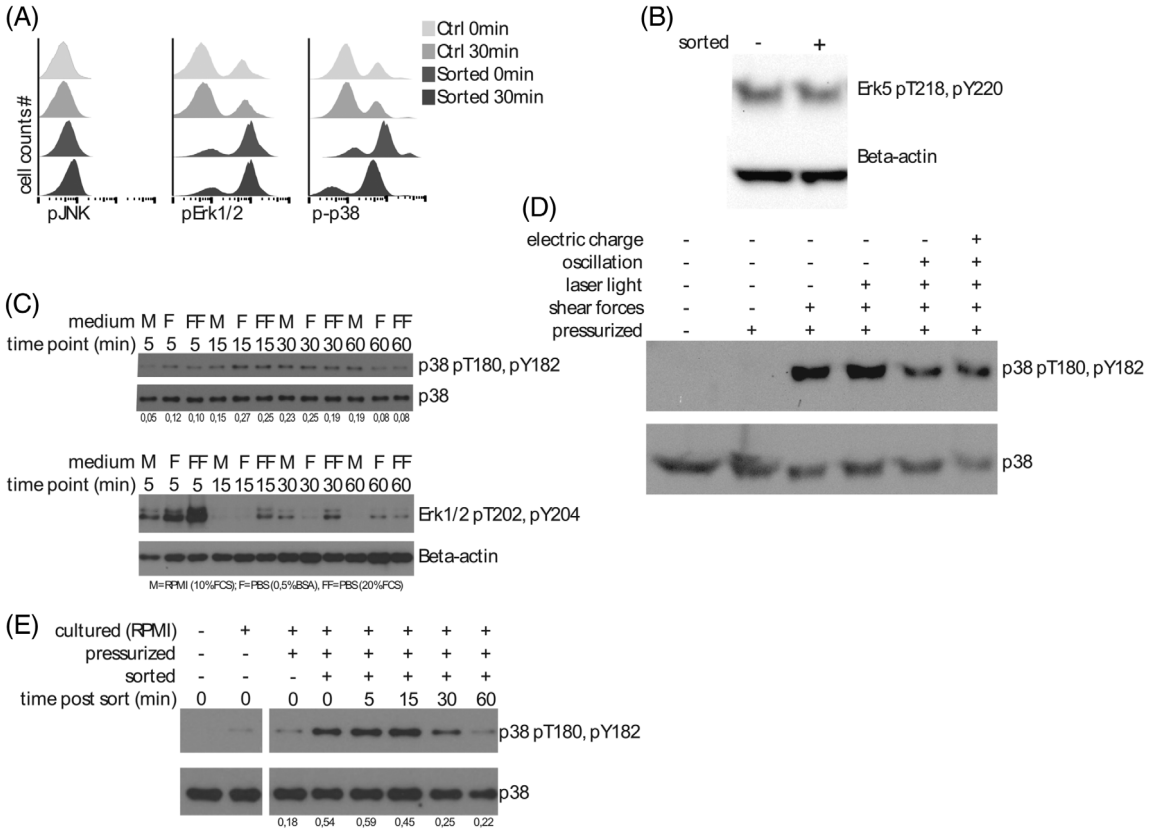

Figure 2. (**A**) Phosphorylation for p38, Erk1/2 and JNK in human PBMCs either "mock" sorted or unsorted (Ctrl.) by flow cytometry. (**B**) Phospho-immunoblot for the MAPK Erk5 in unsorted or "mock" sorted human PBMCs. (**C**) Unsorted human PBMCs tested for sorting buffer induced phosphorylation of p38 and Erk1/2. (**D**) Evaluation of different mechanical and physical sorting parameters on p38 phosphorylation. (**E**) Quantification and time course of cell sorter induced p38 phosphorylation against endogenous p38 levels.

Results

Intracellular Signaling Pathways after Sorting

To screen MAPK activation due to sorting, we abstained from using antibodies and performed sorting on scatter properties only ("mock" sorting). Either human PBMC samples or $CD8^+$ T cells enriched by reversible Fab-TACS® reagents were used and rested overnight (o.N.) beforehand. "Mock" sorting was done on a MoFlo™ XDP (488 nm 200 mW and 355 nm 100 mW lasers). Sorted cells stained with EMA and anti-phosphorylated JNK, Erk1/2, or p38, showed a phosphorylation pattern after "mock" sorting (Fig. 2A) for ERK1/2 and p38 immediately as well as after 30 min. No activation of JNK was detected, although 355 nm laser light was used during sorting, which indicates that the short UV irradiation was not strong enough to activate this pathway. Flow cytometry cell sorting did not induce Erk5 phosphorylation as analyzed by Immunoblot (Fig. 2B).

Sorting buffers imply a potential activation of MAPK by osmolarity, pH changes, or mitogen traces in FCS. To differentiate whether sorting buffers or the instrument induced the observed phosphorylation, the same sample but unsorted was suspended and stored in sorting buffer (Fig. 2C). Transcription factor p38 did not show a sorting buffer-dependent phosphorylation pattern compared to endogenous p38 (calculated by ImageJ). In contrast, the overall phosphorylation of Erk1/2 for buffer containing 20% FCS (FF) was increased. Other buffer conditions did not induce Erk1/2 phosphorylation later than within 5 min. Taken together, only p38 showed pronounced activation due to "mock" sorting, indicating mechanical or physical forces responsible for this activation, so these forces were evaluated for their contribution.

First, sorted samples were pressurized and depressurized with 4 bar which did not induce p38 phosphorylation (Fig. 2D). However, passing cells through a cell sorter fluidic system did activate p38 in PBMCs, either by shear forces or by acceleration. A phosphorylation of p38 due to endotoxins in the sorter or sheath reservoirs was excluded by adding the same volume of sheath buffer to unsorted controls as "mock" sorted. Subsequent forces like oscillation, laser light, electric charge or impact into sorting tubes did not stack to the overall p38 phosphorylation. Rise and decline of phosphorylated p38 signal over time compared to cytoplasmic p38 (Fig. 2E) verified MAPK signaling kinetics. After resting, the p38 activity of the cells leveled out to basic values within 60 min.

Complete Temperature-Controlled Cell Sorting to Avoid p38 Signaling by Hibernation

We next evaluated whether it is possible to avoid p38 activation by cell hibernation during sorting with a fully temperature-

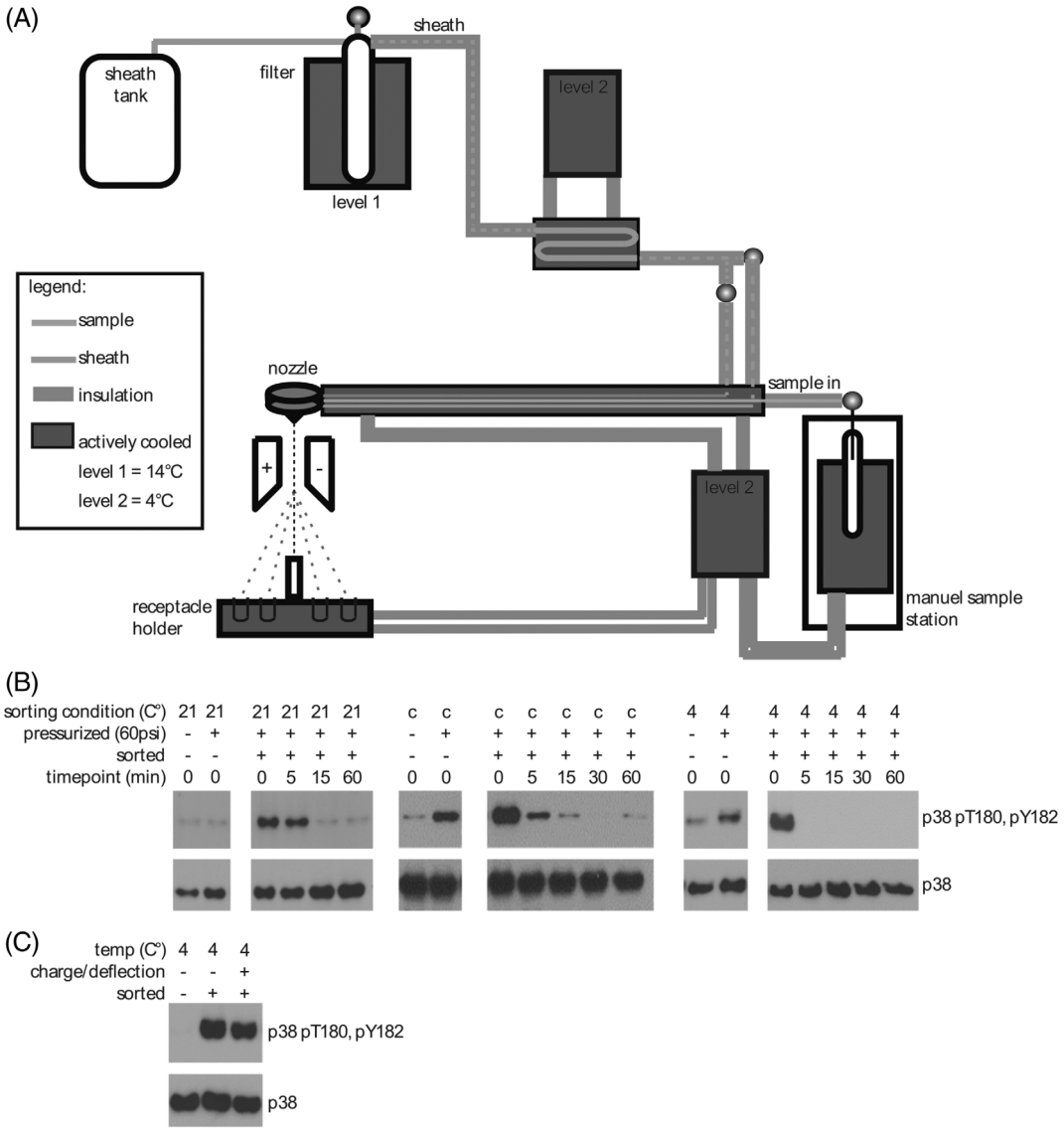

Figure 3. (**A**) Schematic drawing of the changes of the fluidic system of a MoFlo™ XDP. Chillers and insulation enable complete temperature control. Sheath buffer and sample line temperature are freely adjustable. (**B**) Phosphpo-immunoblot of p38 for three different sorting conditions (21°C, 4°C, and conventional (c.) sample chilled, but unchilled sheath buffer) in PBMCs. (**C**) Temperature and sorting influences on PBMCs for p38 activation at 4°C. [Color figure can be viewed at wileyonlinelibrary.com]

controlled sorting approach (Fig. 3A). With certain modifications by insulating all fluidic lines and active chilling of sheath and sample lines, we gained full temperature control of the sorter fluidic system, even within the nozzle assembly. To avoid condensation, a prechilling of the sheath was done to 14°C and in a second step, it was cooled down to 4°C. Also sample and receptacle holder temperature was kept constant at 4°C.

PBMCs "mock" sorted under different temperature conditions led to p38 activation at any given temperature sorting condition (Fig. 3B). Continuous hibernation of PBMCs before and during sorting enhanced early phosphorylation temporarily. However, the phosphorylation was neither induced by 4°C storing conditions nor by deflection or droplet charging (Fig. 3C), while endogenous p38 levels stayed at comparable amounts of protein.

Since no technical variation of sorting conditions could suppress MAPK signaling, cell responses as well as cell alterations (Supporting Information Fig. S1B) induced by the inevitable p38 activation were further elevated.

No Measurable p38-Induced Cell Alterations by "Mock" Sorting

Survival

As p38 phosphorylation potentially influences cell survival, we sorted murine splenocytes on different instruments and evaluated their survival (Fig. 4A) immediately by multiple live/dead markers, which identified late and early apoptotic markers. Flow cytometric cell-sorting gates excluded dead cells by PI staining, but 8–11% of splenocytes were found to

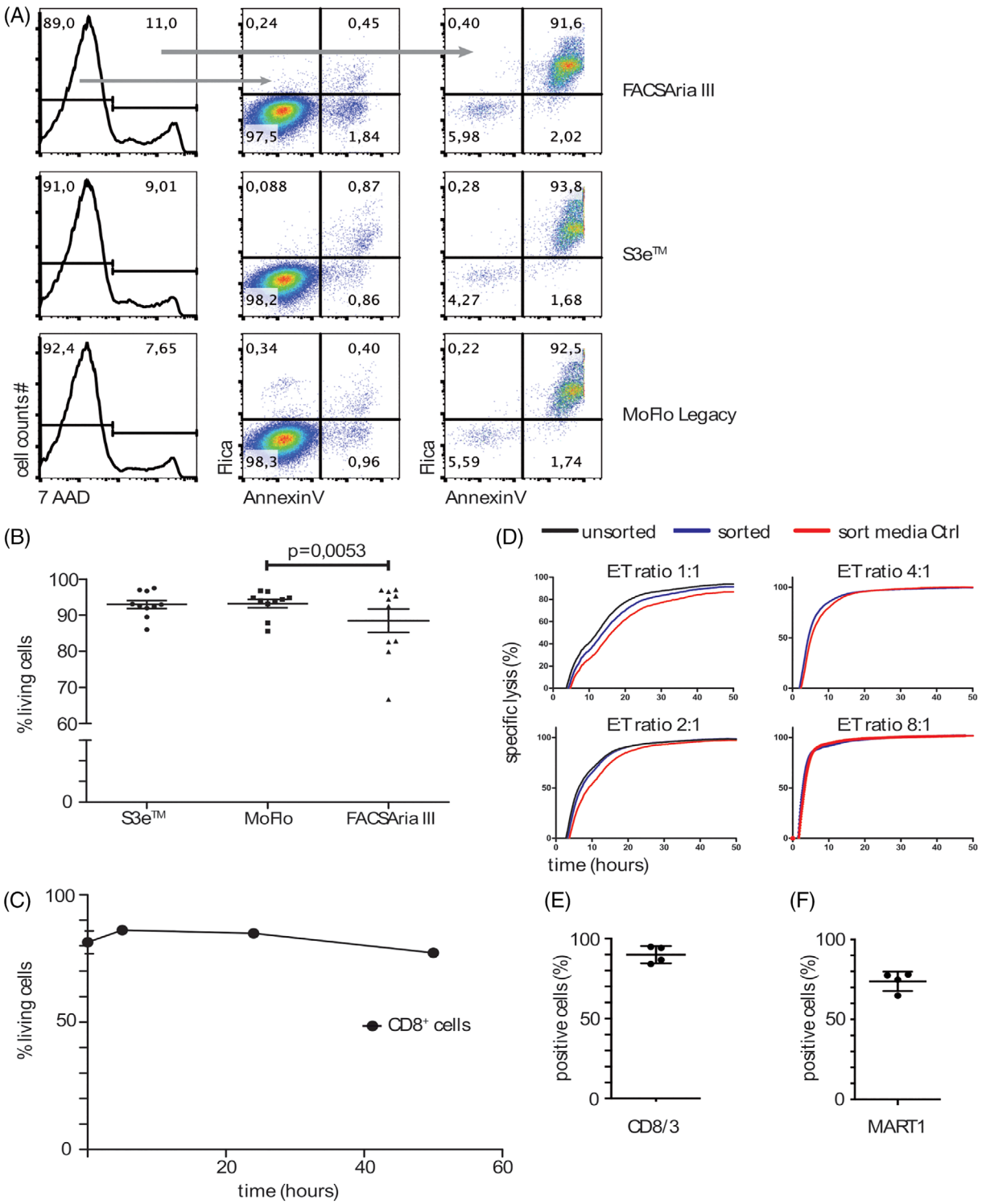

Figure 4. (**A**) Murine splenocytes sorted on different instruments for living lymphocytes and stained afterwards with early (AnnexinV and FLICA) and late (7AAD) apoptotic markers. (**B**) Sorted for living murine splenocytes on three different instruments and analyzed after 2 h' incubation via PI staining by flow cytometry. Pooled data (n = 10) of $CD4^+$ and $CD8^+$ sorted populations. (**C**) Survival of double sorted human $CD8^+$ cells under cell culture conditions (without IL2) over a 2 days' time course. (**D**) One exemplary MART1 antigen specific kill assay (n = 4) with transgenic T cells. A375 cell line was MART1 peptide pulsed. Killing of target cells under different conditions in different E:T ratios was measured with the XCellLigence impedance system. (**E**) Percentage of $CD3^+$ and $CD8^+$ cytotoxic T cells in the impedance assays (n = 4). (**F**) Percentage of antigen specific T cells in the killing assays (n = 4).

be 7AAD-positive immediately after sorting. The FACSAria™ III and S3e™ cell sorter performed similarly, the MoFlo™ system had the highest count for living cells (92.4%). FLICA and AnnexinV staining for double positive early apoptotic cells stood below 1% for all instruments, indicating a low number of cells undergoing apoptotic processes after sorting. AnnexinV-single positive cells from the 7AAD negative compartment were considered as rather disturbed or activated than truly apoptotic.

On the other hand, survival analysis of freshly isolated PBMCs (Supporting Information Fig. 3) purified by flow cytometry or magnetic enrichment showed little more dead cells (97% for unsorted, 96.5% for magnetic and 93.5% for the MoFlo™ system) after purification than unsorted counterparts. However, over a 2-day incubation period, dead and apoptotic cell numbers were equal to unpurified controls, indicating that purification and probably phospho-p38-induced apoptotic cell processes only accelerate dying of a small fraction of cells. The survival of $CD8^+$ T cells isolated from whole blood (Supporting Information Fig. S4) by two sorting steps with a MoFlo™ XDP showed similar numbers and kinetics for PI staining (Fig. 4C) over a 2-day time course, excluding additional ficoll-separation-induced cell death events. In multiple experiments, PI staining was done for murine splenocytes 2 h after sorting (Fig. 4B). For the inter-instrument performance, some differences were detected (p value = 0.0053). However, these differences mainly resulted from few outliers, while most experimental repetitions yielded comparable results.

$CD8^+$ T cell-specific functions after cell sorting

TCR-mediated killing. Like survival, other cellular functions are closely related to cellular fitness, and in the case of T cells, killing via the TCR is one of those and is also related to the p38 MAPK pathway. The capacity of T cells to fulfill their antigen-specific killing potential after cell sorting is a crucial readout system in many *in vitro* and *in vivo* experiments. To evaluate sorting influences on the killing capacity, cell culture-expanded MART1-specific T cells, electropermeabilized to express recombinant TCR, were used in impedance-based killing assay. Transgenic T cells directed against the adherent cell line A-375 and pulsed with the MART1 peptide were used in increasing effector to target ratios. One representative killing assay (n = 4) is shown (Fig. 4D) with normalized curves for target-specific lysis. At high effector-to-target (E:T) ratios like 4:1, no differences between unsorted, sort media control, and "mock" sorted transgenic T cells were visible. At lower E:T ratios, curves between unsorted and sorted cells spread with a lower specific killing for the controls. Effector cells within experiments were 89.97% $CD3^+$ and $CD8^+$ positive (±5.4% standard deviation) (Fig. 4E) of which a large proportion (73.8% ± 6.09) were antigen-specific MART1 transduced T cells (Fig. 4F).

Cell cycle analysis for CD8 T cells after sorting. One main function of p38 is described as a regulator for cell cycle progression (29–31). Therefore, the effect on flow cytometric sorted cells was tested in a mixed lymphocyte reaction. Stimulation with HLA mismatched irradiated cells led to an expansion of $CD8^+$ T cells within the PBMC samples. The proliferation of T cells for different time points, with or without allogeneic stimulus, was measured (Supporting Information Fig. S5A). DNA amplification of cells purified by different methods was compared after 72 h of allogeneic stimulation between flow cytometrically sorted, magnetically purified, and unpurified counterparts (Fig. 5A). While additional CD3 stimulation of effector cells further enhanced proliferation, irradiated stimulator cells alone showed no thymidine uptake. Early data sets correlated closely with each other and showed no significant differences between purified cells and their unpurified controls (Fig. 5B), while a longer time period ranging from 4 to 8 days (Fig. 5C) showed differences. Sorted cells were prone to a faster response to the allogeneic stimulus, which reached a peak of expansion at Day 6 (144 h) with a significantly higher value of "mock" sorted T cells (p = 0.0012) compared to unsorted cells. These data indicate that there is at least no indicator for a cell cycle arrest due to p38 phosphorylation after sorting. However, the longer the allogeneic stimulation persists the more the variability increases within one condition.

Migration of $CD8^+$ T cells after sorting. As the expansion of T cells in a MLR was slightly affected, we further tested influence of sorting on the migration behavior, also associated with p38 signaling in $CD8^+$ T cells. Fresh PBMCs from human blood were stained for CD8 with two different dyes (PE and PB) vice versa to exclude fluorochrome-mediated alteration in migration. In addition, CD4, CD14, CD16, and CD19 staining excluded T helper cells, B cells, monocytes, and other phagocytes (Supporting Information Fig. S5B). Labeling frequencies between "mock" and unsorted cells were adjusted equally, for example, PE 23.1% for "mock" sorted and 25.2% for unsorted or for PB 20.5% for "mock" sorted and 20.9% for unsorted. Migration against a 1% FCS gradient for 4 or 9 h was determined by flow cytometry (Supporting Information Fig. S5C). Even though results varied by staining properties (Fig. 5D), consistent data were achieved by measuring migration in at least six different wells under different labeling conditions and vice versa (Fig. 5E). Nine hours of incubation biased a higher frequency of transmigrated $CD8^+$ T cells labeled with PE due to a better detectability of this dye after longer incubation under cell culture conditions (PB vanishes after 9 h, APC already after 4 h). Analyzed data at all time points and staining conditions did not indicate any impairment in the migratory behavior of $CD8^+$ T cells due to sorting (p = 0.2714). Mainly labeling color and time were affecting the percentage of migrated $CD8^+$ T cells (p < 0.0001).

Cytoskeleton after flow cytometry cell sorting. To further proof unaltered cell migration behavior after sorting, the cell structure proteins tubulin and actin were stained for confocal microscopy. Sorted and unsorted human bladder nonmalignant epithelial cell line HCV-29 (32) (Fig. 5F) and primary cells

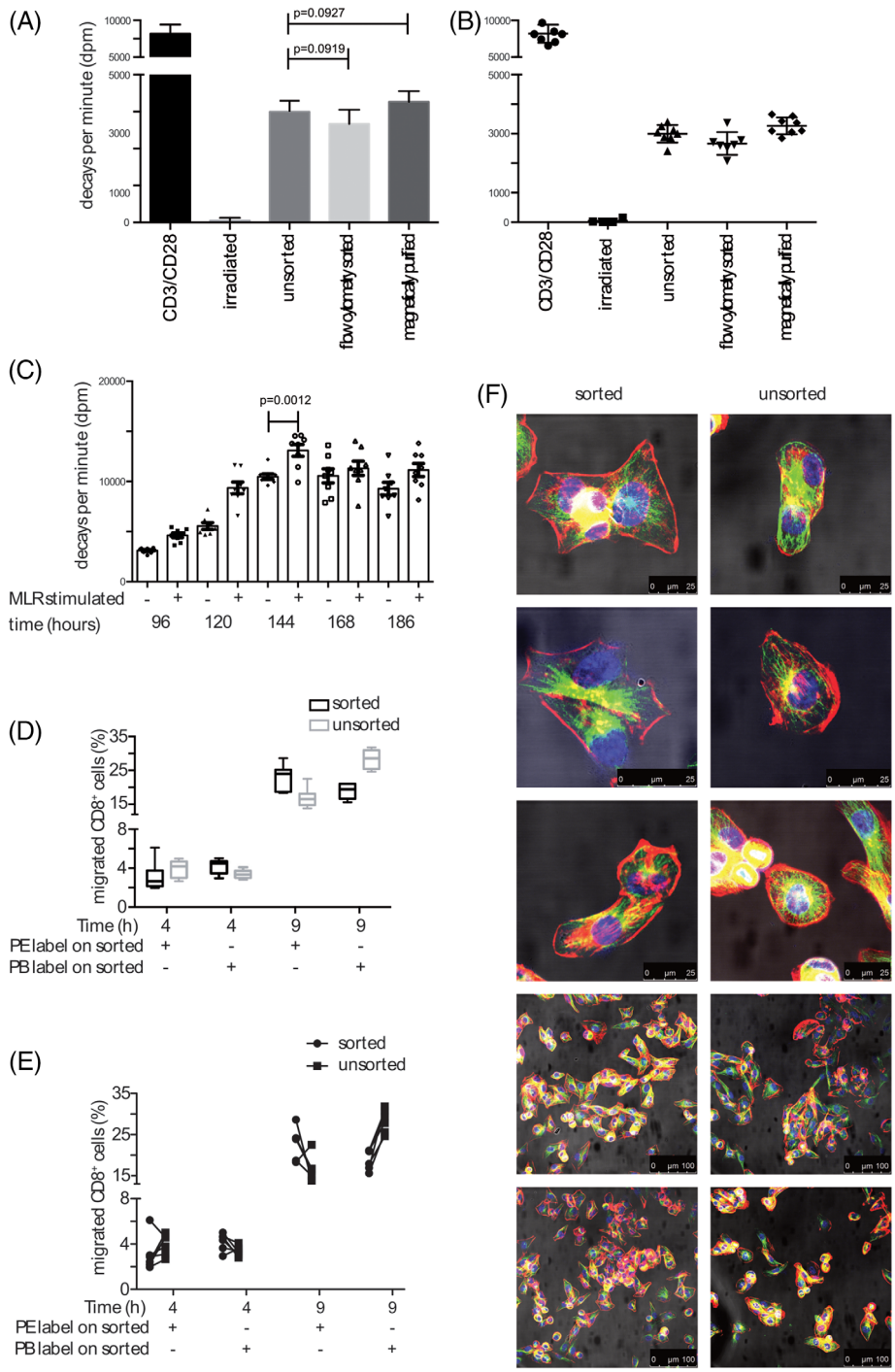

Figure 5. (**A**,**B**) Bar graphs or individual data points (n = 8) of one exemplary experiment for the beta-decay of radioactive H3-labeled thymidine in proliferated CD8$^+$ cells with no significance between unsorted and purified conditions (p = 0.0919 and p = 0.0927). (**C**) Proliferation in a time course (4–8 days) after allogenic stimulation (n = 8) of mock-sorted T cells compared to unsorted (p = 0.0012 at the peak of expansion of around Day 6). (**D**) Transmigration of sorted and unsorted CD8$^+$ T-cells through a 5 nm pore membrane against a 1% FCS gradient. (**E**) Percentage of sorted and unsorted transmigrated CD8$^+$ cells on an intra-well comparison (n = 6). (**F**) Confocal microscopy of cell structure proteins tubulin (green) and actin (red) and the cell nucleus (blue) of "mock" sorted and unsorted HCV-29 cells (32).

(Supporting Information Fig. S6A) were used. In total, nine complete sections were analyzed by six independent investigators comparing sorted against unsorted cells in a blinded study. Representative sections, six cropped in single cell format (40-time ×) and four as complete section are shown. Despite slight morphological changes between cells such as edged shape (beak-like cells) or rounded cell periphery, which were not unique for one condition, observers were not able to identify

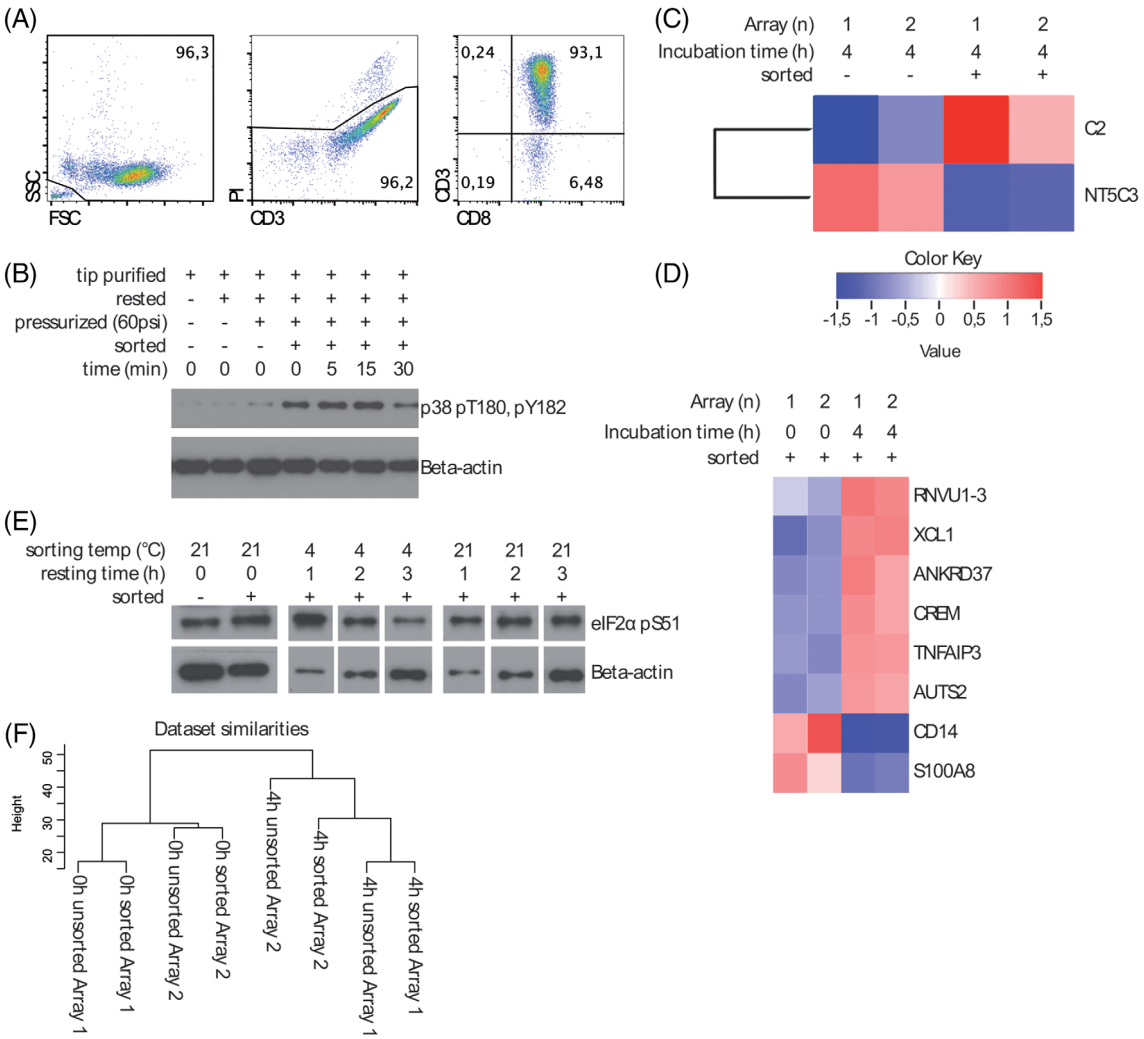

Figure 6. (**A**) From fresh blood enriched Fab-TACS® CD8 enriched cells before MicroArray analysis. (**B**) Immunoblot of Fab-TACS® enriched CD8+ cells for p38 after flow cytometry cell sorting. (**C**) Heatmap of mRNA changes of "mock" sorted Fab-TACS® enriched CD8+ cells compared to unsorted after 4 h ($n = 2$). (**D**) Modified heatmap (exclusion of incubation effects) of differentially regulated mRNA from "mock" sorted Fab-TACS® CD8 cells before and after 4 h of incubation. (**E**) Immunoblot for phosphorylated eIF2α in PBMCs. Sorting and temperature effects under different conditions over a time course were determined. (**F**) Cluster dendrogram ($n = 2$) for the condition similarities within mRNA expression profiles of two independent MicroArrays of Fab-TACS® CD8+ purified human cells.

sorted versus unsorted cells reliably. No deformation or structure ruptures were visible for either tubulin or actin individually (Supporting Information Fig. S7 and S6B).

Transcription analysis for cells after flow cytometry cell sorting. To gain a more complete understanding whether sorter-induced p38 activation was associated with mRNA changes, MicroArray analyses were performed, since a plethora of transcription factors could be involved (Supporting Information Fig. S1B). For comparable results between "mock" and unsorted cells, a pre-enrichment with minimal affected CD8+ T cells isolated out of fresh human donor blood by reversible T catch affinity chromatography (19) Fab-TACS® was done (Supporting Information Fig. S8), yielding more than 96% living cells with purities above 99% CD8+ cells, respectively, >93% CD8+ and CD3+ T cells (Fig. 6A). Cells were given rest overnight and "mock" sorted with a MoFlo™ XDP. mRNA was isolated immediately or after 4 h of incubation in resting medium.

Immunoblot proofed that Fab-TACS® did not affect p38 in cells before MicroArray analysis (Fig. 6B), and "mock" sorting generated a pronounced phosphorylation. Despite this, only little effect on mRNA levels was found after sorting. We compared the changes between "mock" and unsorted populations immediately after the sorting process (Supporting Information Fig. S2B). Here, only two genes out of 18,710 mRNA data sets, C2 and IGHG1, were twofold down-regulated. Comparable changes were visible between "mock" and unsorted after a 4 h resting phase (Fig. 6C). After normalization, two mRNA profiles remained differentially

expressed by factor 2. In sorted cells, complement component 2 (C2) was overexpressed, 5'-nucleotidase, and cytosolic IIIA (NT5C3) was downregulated. Interestingly, C2 was also downregulated in "mock" sorted at time point zero (Supporting Information Fig. S2B), indicating an increase of this mRNA in sorted cells after the resting phase. C2 acts as part of the classical and lectin pathway in complement activation (33) and is essential to activate C3, the gatekeeper in the complement pathway (34). As a plasma protein physiologically produced in the liver, it is not likely to be specifically regulated by the p38 activation of PBMCs by sorting. More likely, the enrichment of some $CD8^+$ DCs after Tip purification might be the cause for this finding. Previous work already showed increased mRNA levels of C2 for different macrophages under stress and in inflammatory conditions (35).

In contrast, more gene-expression profiles differed between the cells after 4 h resting phase in both unsorted and "mock" sorted controls (Supporting Information Fig. S2C,D). To exclude changes induced by the resting period, we generated a heatmap adjusted for differentially expressed genes after 4 h compared to unsorted groups (Fig. 6D). This approach resulted in eight mRNAs of which six were upregulated and two downregulated. Seven of those were protein coding, with exception for RNA variant U1 small nuclear 1, 2, and 3 (RNVU1-3), which is coding for snRNA. The X-C motif chemokine ligand 1 (CML), TNF alpha induced protein 3 (TNFAIP3), and the S100 calcium binding protein A8 could be regulated by transcription factors associated with p38 signaling. Cyclic adenosine monophosphate (cAMP)-responsive-element-modulator (CREM) could be linked to a stress response via eIF2α phosphorylation. However, we found no activation of eIF2α in sorted samples, which would induce a translation stop of mRNA to protein (Fig. 6E). Only sorting at 4°C induced some eIF2α phosphorylation.

The comparison of overall mRNA profiles within the assay was analyzed in a cluster dendrogram (Fig. 6F), graphically displaying data set similarities in a hierarchical tree. mRNA profiles between the incubation times accounted for the greatest differences. Of all conditions, "mock" sorting induced the smallest effect on mRNA levels. However, with only seven differentially expressed genes the differences are too minor to identify enrichments or correlations between the analyzed samples.

Discussion

In this study, we analyzed the potential impact of flow cytometry cell sorting on subsequent cell functions. Despite demonstration of sorter-induced MAPK p38 activation, detectable cell changes by flow cytometry cell sorting were only minor and did not indicate any significant changes of cellular readouts. In order to analyze instrument-based influences, it was important to use defined cell material that was as little disturbed as possible. We addressed this in different ways. First, we applied technologies available to generate highly defined, pure, minimally manipulated cell populations by reversible staining and isolation out of fresh whole blood via FabTACS®, as already shown by other groups (36,37). Second, we preferentially used human primary blood cells to reduce artifacts generated by immortalized or cultured cells of sometimes unknown origin (38–41). Immortalized cells show high intrinsic activity, for example, the MAPK pathway can be inhomogeneously activated due to high cell division rates. We therefore preferred primary lymphocytes from humans or mice, although we were aware that sample preparation like density purification or homogenization of organs still can influence experimental outcome. For the separation of cells by Ficoll–Hypaque solution, no major cell phenotypic changes have been described, but a loss of certain cell types is known (42,43). In order to exclude Ficoll-influences for our experiments, we tested sample material before all assays, especially when intracellular signaling pathways or mRNA-levels were evaluated.

We controlled sort parameters such as temperature, pressure, buffers, laser light or charging and deflection independently and thereby generated a unique experimental platform to evaluate the influence of these parameters on sorted cells.

The sorter-induced phosphorylation of the MAPK pathways for p38 and in parts also for Erk1/2 reflects a cellular stress sensing most likely induced by parameters like acceleration or shearing of cells, forces unavoidable due to the instrument design. Yet, in contrast to previous reports (44,45), the cellular sensing was not accompanied by detectable cellular stress responses. However, other methods like detection of mitochondrial reactive oxygen species (mROS) stress responses (46) or inhibition of the p38 dephosphorylation by MAPK phosphatases (MKPs) might provide additional insights and therefore we cannot fully exclude minor sorter-induced cellular stress responses or an inhibition of the p38 dephosphorylation as cellular responses to sorting.

Although some differences were measured, for example, in proliferation or killing, no functional impairment of sorted cells was detected. After sorting, PBMCs proliferated even faster at later time points. Viability was dependent on the instrument and up to 10 % of sorted cells had a structural loss of membrane integrity. However, the cells that survived cell sorting did not undergo apoptosis and analysis at later time points (up to 2 days) showed comparable results between sorted and unsorted.

Cell death immediately after cell sorting, as identified by PI or 7AAD staining, indicated a membrane rupture to some extent. The cytoskeleton coordination between sorted and unsorted living cells never gave hints of rupture of actin nor tubulin. In line with this, the migratory potential of cells, which is strongly associated with cellular structure proteins, was not impaired by sorting.

We assume that cell sorting could accelerate the death of cells, which were already prone to die before the sorting process.

The p38 phosphorylation induced little to no changes in mRNA expression profiles. Cluster dendrogram analysis indicated the closest relation between sorted and unsorted

samples. Taken together, these studies indicate that cells are capable of sensing the sorting by their molecular signaling machinery; yet, these stimuli seem insufficient to change cellular behavior, physiology or function, at least for primary cells.

Many published experiments using flow cytometric cell sorting relied on a low technical bias of the sorting process, especially susceptible read out systems like RNA-seq, MicroArrays, or quantitative PCR without controlling for this potential experimental influences.

In this context, our data support the interpretation that sorting itself causes only minor changes to the isolated cells. However, we are aware that primary $CD8^+$ T cells might not be the most sensitive cell type to react within 4 h to changes in the extrinsic environment and sorter induced forces.

Our temperature-controlled cell sorting approach in combination with reversible dyes could become important to guarantee unaltered readouts when antibodies are used in sorting.

Acknowledgments

This work was in part funded by the Deutsche Forschungsgemeinschaft (DFG, German Research Foundation) – "Projektnummer 272983813" – TRR 179. The authors thank Philipp Bruns (DKFZ, Heidelberg) and Lena Appel (MIH, München) for help with data processing and visualization of MicroArray data.

Author contributions

I.A. wrote the manuscript, designed and performed experiments and analyzed data. H.U., S.D., and D.S. performed experiments and analyzed data. L.H., C.A., and J.R. performed experiments. S.P., H.S., and M.E. provided key technologies. D.H.B. and M.S. supervised coordination and financing of the research project, co-wrote manuscript, provided methodological and scientific input and lab infrastructure.

Literature Cited

1. Saba-El-Leil MK, Fremin C, Meloche S. Redundancy in the world of MAP kinases: All for one. Front Cell Dev Biol 2016;4:67. https://doi.org/10.3389/fcell.2016.00067
2. Nishimoto S, Nishida E. MAPK signalling: ERK5 versus ERK1/2. EMBO Rep 2006; 7:782–786. https://doi.org/10.1038/sj.embor.7400755
3. Donnelly N, Gorman AM, Gupta S, Samali A. The eIF2alpha kinases: Their structures and functions. Cell Mol Life Sci 2013;70(3):493–3,511. https://doi.org/10.1007/s00018-012-1,252-6
4. Stemberger C, Huster KM, Koffler M, Anderl F, Schiemann M, Wagner H, Busch DH. A single naive CD8+ T cell precursor can develop into diverse effector and memory subsets. Immunity 2007;27:985–997. https://doi.org/10.1016/j.immuni.2007.10.012
5. Graef P, Buchholz VR, Stemberger C, Flossdorf M, Henkel L, Schiemann M, Drexler I, Höfer T, Riddell SR, Busch DH. Serial transfer of single-cell-derived immunocompetence reveals stemness of CD8(+) central memory T cells. Immunity 2014;41:116–126. https://doi.org/10.1016/j.immuni.2014.05.018
6. Stemberger C, Neuenhahn M, Buchholz VR, Busch DH. Origin of CD8+ effector and memory T cell subsets. Cell Mol Immunol 2007;4:399–405.
7. Zhou X, Naguro I, Ichijo H, Watanabe K. Mitogen-activated protein kinases as key players in osmotic stress signaling. Biochim Biophys Acta 2016;1860:2037–2052. https://doi.org/10.1016/j.bbagen.2016.05.032
8. Pasantes-Morales H, Lezama RA, Ramos-Mandujano G, Tuz KL. Mechanisms of cell volume regulation in hypo-osmolality. Am J Med 2006;119:S4–S11. https://doi.org/10.1016/j.amjmed.2006.05.002
9. Burg MB, Ferraris JD, Dmitrieva NI. Cellular response to hyperosmotic stresses. Physiol Rev 2007;87(1):441–1474. https://doi.org/10.1152/physrev.00056.2006
10. Wang L, Wormstone IM, Reddan JR, Duncan G. Growth factor receptor signalling in human lens cells: Role of the calcium store. Exp Eye Res 2005;80:885–895. https://doi.org/10.1016/j.exer.2005.01.002
11. Nicolini C, Baserga R, Kendall F. DNA structure in sheared and unsheared chromatin. Science 1976;192:796–798.
12. Richardson GM, Lannigan J, Macara IG. Does FACS perturb gene expression? Cytometry 2015;87A:166–175. https://doi.org/10.1002/cyto.a.22608
13. Kazi M, Lundmark K, Religa P, Gouda I, Larm O, Ray A, Swedenborg J, Hedin U. Inhibition of rat smooth muscle cell adhesion and proliferation by non-anticoagulant heparins. J Cell Physiol 2002;193:365–372. https://doi.org/10.1002/jcp.10184
14. Schwab R, Crow MK, Russo C, Weksler ME. Requirements for T cell activation by OKT3 monoclonal antibody: Role of modulation of T3 molecules and interleukin 1. J Immunol 1985;135(1):714–1,718.
15. Dyavar Shetty R, Velu V, Titanji K, Bosinger SE, Freeman GJ, Silvestri G, Amara RR. PD-1 blockade during chronic SIV infection reduces hyperimmune activation and microbial translocation in rhesus macaques. J Clin Invest 2012;122(1): 712–1,716. https://doi.org/10.1172/JCI60612
16. Melero I, Shuford WW, Newby SA, Aruffo A, Ledbetter JA, Hellström KE, Mittler RS, Chen L. Monoclonal antibodies against the 4-1BB T-cell activation molecule eradicate established tumors. Nat Med 1997;3:682–685.
17. Moreau JL, Nabholz M, Diamantstein T, Malek T, Shevach E, Thèze J. Monoclonal antibodies identify three epitope clusters on the mouse p55 subunit of the interleukin 2 receptor: Relationship to the interleukin 2-binding site. Eur J Immunol 1987; 17:929–935. https://doi.org/10.1002/eji.1830170706
18. Goding JW. Biological effects of antibodies to lymphocyte surface receptors. Springer Semin Immunopathol 1982;5:463–475.
19. Stemberger C, Dreher S, Tschulik C, Piossek C, Bet J, Yamamoto TN, Schiemann M, Neuenhahn M, Martin K, Schlapschy M, et al. Novel serial positive enrichment technology enables clinical multiparameter cell sorting. PLoS one 2012; 7:e35798. https://doi.org/10.1371/journal.pone.0035798
20. Knight JR, Bastide A, Roobol A, Roobol J, Jackson TJ, Utami W, Barrett DA, Smales CM, Willis AE. Eukaryotic elongation factor 2 kinase regulates the cold stress response by slowing translation elongation. Biochem J 2015;465:227–238. https://doi.org/10.1042/BJ20141014
21. Roberts JR, Rowe PA, Demaine AG. Activation of NF-kappaB and MAP kinase cascades by hypothermic stress in endothelial cells. Cryobiology 2002;44:161–169.
22. Stanciu LA, Shute J, Holgate ST, Djukanovic R. Production of IL-8 and IL-4 by positively and negatively selected CD4+ and CD8+ human T cells following a four-step cell separation method including magnetic cell sorting (MACS). J Immunol Methods 1996;189:107–115.
23. Sao H, Kitaori K, Kasai M, Shimokawa T, Kato C, Yamanishi H, Ueda R, Morishima Y. A new marrow T cell depletion method using anti-CD6 monoclonal antibody-conjugated magnetic beads and its clinical application for prevention of acute graft-vs.-host disease in allogeneic bone marrow transplantation: Results of a phase I-II trial. Int J Hematol 1999;69:27–35.
24. Watanabe N, Kamachi Y, Koyama N, Hama A, Liang J, Nakamura Y, Yamamoto T, Isomura M, Kudo K, Kuzushima K, et al. Expansion of human CMV-specific cytotoxic T lymphocytes to a clinical scale: A simple culture system using tetrameric HLA-peptide complexes. Cytotherapy 2004;6:514–522. https://doi.org/10.1080/14653240410005005
25. Hoffmann P, Boeld TJ, Eder R, Albrecht J, Doser K, Piseshka B, Dada A, Niemand C, Assenmacher M, Orsó E, et al. Isolation of CD4 + CD25+ regulatory T cells for clinical trials. Biol Blood Marrow Transplant 2006;12:267–274. https://doi.org/10.1016/j.bbmt.2006.01.005
26. Varma S, Fendyur A, Box A, Voldman J. Multiplexed cell-based sensors for assessing the impact of engineered systems and methods on cell health. Anal Chem 2017;89(4):663–4,670. https://doi.org/10.1021/acs.analchem.7b00256
27. World Medical Association. World Medical Association Declaration of Helsinki: Ethical principles for medical research involving human subjects. JAMA 2013;310: 2191–2194. https://doi.org/10.1001/jama.2013.281053
28. Giard DJ, Aaronson SA, Todaro GJ, Arnstein P, Kersey JH, Dosik H, Parks WP. In vitro cultivation of human tumors: Establishment of cell lines derived from a series of solid tumors. J Natl Cancer Inst 1973;51(1):417–1,423.
29. Duch A, de Nadal E, Posas F. The p38 and Hog1 SAPKs control cell cycle progression in response to environmental stresses. FEBS Lett 2012;586(2):925–2,931. https://doi.org/10.1016/j.febslet.2012.07.034
30. Thornton TM, Rincon M. Non-classical p38 map kinase functions: Cell cycle checkpoints and survival. Int J Biol Sci 2009;5:44–51.
31. Coulthard LR, White DE, Jones DL, McDermott MF, Burchill SA. p38(MAPK): Stress responses from molecular mechanisms to therapeutics. Trends Mol Med 2009;15:369–379. https://doi.org/10.1016/j.molmed.2009.06.005
32. Hisazumi H, Andersson L, Collins VP. Fibrinolytic activity of in vitro cultivated human bladder cell lines. Urol Res 1977;5:133–139.
33. Matsushita M, Endo Y, Fujita T. Structural and functional overview of the lectin complement pathway: Its molecular basis and physiological implication. Arch Immunol Ther Exp 2013;61:273–283. https://doi.org/10.1007/s00005-013-0229-y
34. Sim RB, Tsiftsoglou SA. Proteases of the complement system. Biochem Soc Trans 2004;32:21–27.
35. Luo C, Chen M, Madden A, Xu H. Expression of complement components and regulators by different subtypes of bone marrow-derived macrophages. Inflammation 2012;35(1):448–1,461. https://doi.org/10.1007/s10753-012-9,458-1
36. Pelak O, Kužílková D, Thürner D, Kiene ML, Stanar K, Stuchlý J, Vášková M, Starý J, Hrušák O, Stadler H, et al. Lymphocyte enrichment using CD81-targeted immunoaffinity matrix. Cytometry 2017;91A:62–72. https://doi.org/10.1002/cyto.a.22918
37. Mohr F, Fischer JC, Nikolaus M, Stemberger C, Dreher S, Verschoor A, Haas T, Poeck H, Busch DH. Minimally manipulated murine regulatory T cells purified by

reversible Fab Multimers are potent suppressors for adoptive T-cell therapy. Eur J Immunol 2017;47(2):153–2,162. https://doi.org/10.1002/eji.201747137

38. Pan C, Kumar C, Bohl S, Klingmueller U, Mann M. Comparative proteomic phenotyping of cell lines and primary cells to assess preservation of cell type-specific functions. Mol Cell Proteomics 2009;8:443–450. https://doi.org/10.1074/mcp.M800258-MCP200
39. Alge CS, Hauck SM, Priglinger SG, Kampik A, Ueffing M. Differential protein profiling of primary versus immortalized human RPE cells identifies expression patterns associated with cytoskeletal remodeling and cell survival. J Proteome Res 2006;5:862–878. https://doi.org/10.1021/pr050420t
40. Alge CS, Suppmann S, Priglinger SG, Neubauer AS, May CA, Hauck S, Welge-Lussen U, Ueffing M, Kampik A. Comparative proteome analysis of native differentiated and cultured dedifferentiated human RPE cells. Invest Ophthalmol Vis Sci 2003;44(3):629–3,641. https://doi.org/10.1167/iovs.02-1,225
41. Lorsch JR, Collins FS, Lippincott-Schwartz J. Cell biology. Fixing problems with cell lines. Science 2014;346(1):452–1453. https://doi.org/10.1126/science.1259110
42. Tamul KR, Schmitz JL, Kane K, Folds JD. Comparison of the effects of Ficoll–Hypaque separation and whole blood lysis on results of immunophenotypic analysis of blood and bone marrow samples from patients with hematologic malignancies. Clin Diagn Lab Immunol 1995;2:337–342.
43. De Paoli P, Villalta D, Battistin S, Gasparollo A, Santini G. Selective loss of OKT8 lymphocytes on density gradient centrifugation separation of blood mononuclear cells. J Immunol Methods 1983;61:259–260.
44. Mollet M, Godoy-Silva R, Berdugo C, Chalmers JJ. Acute hydrodynamic forces and apoptosis: A complex question. Biotechnol Bioeng 2007;98:772–788. https://doi.org/10.1002/bit.21476
45. Mollet M, Godoy-Silva R, Berdugo C, Chalmers JJ. Computer simulations of the energy dissipation rate in a fluorescence-activated cell sorter: Implications to cells. Biotechnol Bioeng 2008;100:260–272. https://doi.org/10.1002/bit.21762
46. Llufrio EM, Wang L, Naser FJ, Patti GJ. Sorting cells alters their redox state and cellular metabolome. Redox Biol 2018;16:381–387. https://doi.org/10.1016/j.redox.2018.03.004